INFORMATION REDACTED PURSUANT TOTHE FREEDOM
OF INFORMATION ACT (FOIA), 5 U.S.C.552(B)(6)

AES 12128282-5-1
January 2013

Failure Analysis of the Power Spring of a Spring Brake Chamber

Prepared By

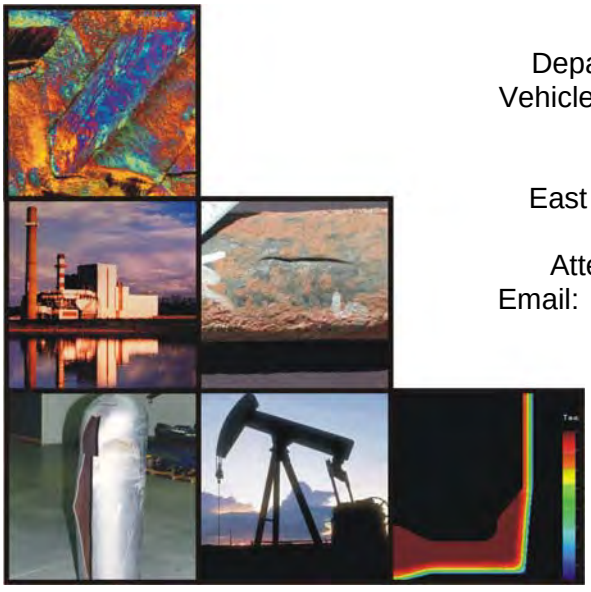
Benjamin K. Jackson, Ph.D.

Intertek AIM

Prepared For

Department of Transportation
Vehicle Research and Test Center
PO Box B-37
10820 SR 347
East Liberty, OH 43319-0337

Attention: Mr. Dan Pearse
Email: dan.pearse@nhtsa.dot.gov



Intertek AIM
601 W. California Avenue, Sunnyvale, CA 94086, 408.745.7000
16100 Cairnway Drive, Suite 310 , Houston, TX 77084, 832.593.0550
www.intertek.com/aim

This report was prepared by Intertek AIM as an account of work sponsored by the organization named herein. Neither Intertek AIM nor any person acting on behalf of Intertek AIM: (a) makes any warranty, express or implied, with respect to the use of any information, apparatus, method, or process disclosed in this report or that such use may not infringe privately owned rights; or (b) assumes any liabilities with respect to the use of, or for damages resulting from the use of, any information, apparatus, method, or process disclosed in this report.

FAILURE ANALYSIS OF THE POWER SPRING OF A SPRING BRAKE CHAMBER

BACKGROUND

Intertek AIM was asked by the U. S. Department of Transportation (U.S. DOT) Vehicle Research and Test Center (VRTC) to perform an independent failure analysis to determine the root cause of failures in polymer coated power springs in spring brake chambers. The chambers are used on heavy construction equipment and trucks to actuate the parking brake.

The samples obtained by the VRTC consisted of ex-service spring brake chambers that were removed from trucks as part of routine maintenance. The service conditions (number of cycles, operating environment, etc.) were not known. The springs were then taken to failure in their in-lab test frames.

Two samples of power springs were supplied, labeled 76071 and 78137. The chambers from which they had been extracted had VIN per MGM #1 and MGM #2, respectively. The chambers were of Type 30LP3. The chambers were cycled to failure in the VRTC lab test frames. Failure was designated as the point at which air leakage at the diaphragm prevented further operation of the chamber. Multiple fractures may occur along the length of the power spring before the diaphragm finally ruptures.

Further details of the number of cycles to failure and the number of spring breaks that occurred for Chambers 76071 and 78137 can be found in Table 1.

Intertek AIM was requested to investigate the laboratory failed springs, and to compare/contrast their failure mechanism(s), material composition, microstructure, and state of the polymeric surface coating to that of the Haldex spring brake chambers previously investigated (Intertek AIM Report AES 12058074-5-1, May 2012). Intertek AIM was also asked to determine if the surface of the spring had been hardened with respect to the core of the spring wire.

The following samples were provided to Intertek AIM in a vacuum desiccator chamber for analysis:

- Three sections and two mounted and ground cross-sections of power spring labeled 78137. Two of the sections were mating fracture surfaces (A and B). One ~2 cm long section from an un-failed region in the spring was to be used for chemical compositional analysis. Finally, the two mounted cross-sections from an un-failed region of the spring (-1 and -2) were to be used for metallography and hardness testing.
- Seven sections and two mounted and ground cross-sections of power spring labeled 76071. Six of the sections were mating fracture surfaces (A – F). One ~2 cm long section from an un-failed region in the spring was to be used for chemical compositional analysis. Finally, the two mounted cross-sections from an un-failed region of the spring (-1 and -2) were to be used for metallography and hardness testing.

VISUAL EXAMINATION

Images of the as-received samples are shown in Figures 1 and 2. Figure 2 is an image provided by VRTC detailing the multiple fracture locations in Sample 76071. Sample 78137 contained only a single fracture.

Figures 3 through 11 show images of the as-received fracture surfaces individually for both samples.

Initial observations of the samples are as follows:

- The polymer coating (referred to as simply “paint” hereon) is only present in patches on the surface of the segments provided. The metal exposed where the paint is not present appears to be oxidized and pitted. The likely cause of the corrosion was interaction with the potentially wet and corrosive (e.g., road salt) environment that the vehicle was subjected to in service. The brake chambers are not sealed from the external environment, potentially allowing corrosion of the unprotected regions of the spring where the paint has separated from the spring steel. Further corrosion of the surface of

the spring by the external environment caused oxidation of the spring surface. The increased volume taken by the oxide at the paint/spring interface caused further separation of the paint from the spring surface, increasing the area of spring steel left uncoated.

- The fracture surfaces are, in general, not oxidized, with the exception of isolated regions on a few of the samples. This suggests that the majority of the crack propagation occurred during the lab testing in a controlled (dry) environment over a relatively short amount of time (compared to service life required for failure). The oxidized areas were likely exposed during service and were present prior to laboratory testing.

- Some of the fracture surfaces show a black deposit toward the outer diameter (OD) of the spring sections.

- Some of the fracture surfaces show shiny, smooth areas consistent with wear on both the OD surface and isolated regions (high points) of the fracture surfaces.

- All fracture surfaces appear to be made up mostly of torsional fatigue, with an initiation point at the OD surface of the spring section consistent with an area lacking in paint.

FRACTOGRAPHY

A representative set of fracture surfaces from Sample 76071 (A, D, E, F, G) and the A side of Sample 78137 were selected for more detailed fractographic analysis. The samples that showed the possibility of in-service cracking were selected (those showing oxidation at/on the fracture surface). The following is a summary of the analyses for each selected fracture surface:

- 76071 A (Figures 12 and 13):

    - Two likely origins visible on the OD of the spring. One appears to be a point source emanating from a corrosion pit in a region where there is a lack of paint. The other appears to be a small axially-oriented crack, again initiated from a region on the OD corresponding to corrosion and a lack of paint.

- Oxidation of the fracture surfaces emanating from the initiation points suggests that oxidation was present during the time the spring was in service, and was likely present at the beginning of the laboratory testing.

- The crack fronts initiated at the two neighboring origin sites combined and progressed through the spring section during the load/unload cycles of the spring. The primary failure mode is torsional fatigue. The shear lips in the figures represent the regions of final fracture.

- Areas of shiny and smooth material are evident on the edges of the fracture surface. This is likely due to wear with the B side of the fracture after failure had occurred. The lab test was run until the diaphragm ruptured and was not stopped upon the first spring failure. The wear marks were likely a result of the two spring sections rubbing together while held loosely in place during the remainder of the test. It is also possible that the broken spring sections could have made contact with the interior parts of the brake chamber. The remainder of the chamber was not supplied to Intertek AIM for evaluation, so this cannot be confirmed.

■ 76071 D (Figures 14 and 15):

- One distinct primary and one possible secondary origin at the spring OD.

- These origins correspond to areas with a lack of paint and some corrosion in the form of pits.

- The primary origin appears to have been initiated from a corrosion pit, showing classic markings pointing back to the initiation site at the base of a pit on the OD. The remainder of the fracture surface showed that the spring failed by torsional fatigue.

- Little corrosion was observed on the fracture surface, indicating that this failure likely propagated almost entirely in the lab. However, the corrosion pit from which the crack initiated was most likely due to in-service corrosion, as observed in the other spring samples.

- Black deposits were observed on the outer edges of the fracture surface. Break D was from a portion of the spring that was at its widest diameter (the intact spring had

a “beehive” shape). It is possible that the sharp edges of the fracture surface impacted the interior walls of the brake chamber housing during the portion of the lab testing post-fracture of the spring but pre-fracture of the diaphragm, transferring material from the chamber wall onto the fracture surface. This is supported by the chemical analysis performed (details in a subsequent report section) on this spring surface that identified the presence of aluminum (Al) and a small amount of silicon (Si) and oxygen (O) in the black deposit. The brake chamber was made of aluminum, and was oxidized according to VRTC observations. Silicon could conceivably be present inside the chamber from road or work site debris that entered the chamber in service.

- 76071 E, F, and G (Figures 16 through 18):

  - These three fracture surfaces are all grouped together as they appear to have all initiated from the same area.

  - The initiation site is best displayed on Surface F. The highly oxidized region at the top of the surface (Figure 17) shows a pair of origins at corrosion pits on the OD, corresponding to a region of the spring surface where there is a lack of paint and significant surface pitting corrosion.

  - Surface F is heavily oxidized (compared to all the other fracture surfaces supplied), suggesting that the crack had been exposed during service. The extent to which the oxidation has spread (almost to the core of the spring) suggests that this fracture had been exposed for the longest time in service, and it is likely that this multiple fracture was the first to occur during lab testing.

  - The crack front initiated from the OD corrosion pits, then initiated two torsional fatigue failures (E-F and G-F) to produce the three sections supplied.

  - Areas of shiny and smooth material are evident on the edges of the fracture surface in G and to some extent in F and E. This is likely due to wear with the other sides of the fractures after failure had occurred. The lab test was run until the diaphragm ruptured, and was not stopped upon the first spring failure. The wear marks were likely a result of the two spring sections rubbing together while held loosely in place during the remainder of the test. It is also possible that the broken spring sections

could have made contact with the interior parts of the brake chamber. The remainder of the chamber was not supplied to Intertek AIM for evaluation, so this cannot be confirmed.

- 78137 A (Figures 19 and 20):

  - Two likely origins were visible on the OD of the spring. One appears to be a point source emanating from a corrosion pit in a region where there is a lack of paint. The other appears to be a small axially-oriented crack, again initiated from a region on the OD corresponding to heavy pitting corrosion and a lack of paint.

  - Oxidation of the fracture surfaces emanating from the initiation points suggests that the oxidation was present during the time the spring was in service, and was likely present at the beginning of the laboratory testing. Oxidation surrounding the axially-oriented crack extends ~1/3 of the spring diameter from the surface to the core, suggesting that this was the primary initiation point of the failure.

  - Multiple ratchet marks are present adjacent to the primary origins. This suggests possible secondary initiation points, which are again associated with a corrosion pit on the surface of the spring.

  - The crack fronts initiated at the two neighboring origin sites combined and progressed through the spring section during the load/unload cycles of the spring. The primary failure mode is torsional fatigue. The shear lips in the figures represent the regions of final fracture.

  - There are isolated areas of shiny material at the edges of the fracture surface. This is likely due to wear caused by contact with the adjacent fracture surface (B) or with the interior of the chamber wall post-fracture of the spring, but pre-fracture of the diaphragm.

  - Each of the springs examined in this analysis appeared to have failed by torsional fatigue from initiation points (point flaws or liner cracks) initiated from one or more corrosion pits on the OD surface in areas corresponding to a lack of paint and light-to-severe corrosion of the underlying steel surface. These observations are consistent with the failure modes observed for the Haldex springs.

MICROSTRUCTURAL ANALYSIS

Figures 21 and 22 show the microstructure of the spring steel for both samples. The cross-sectional samples supplied were used to prepare these micrographs. Samples were etched in 4% nital to give optical contrast to the microstructure.

Micrographs are taken both at the core of the spring and at the edge. The micrographs all show a typical lightly tempered martensitic structure.

To compare this to the Haldex springs, the manufacturer's Specification NS-65-99, Section 3.8.1 specifies that the microstructure of the spring material:

> "… shall exhibit a fine homogeneous tempered martensitic structure free from ferrite, intermediate transformation products, and/or detrimental inclusions."

Both of the current samples are consistent with the specified microstructure of the Haldex springs.

HARDNESS TESTING

Intertek AIM was asked to check for evidence of a surface hardening treatment on the samples provided (shot peening, case hardening, etc.).

In order to investigate the presence of a surface hardened layer, a microhardness traverse was performed. Figures 23 and 24 show the detail of the traverses for Sample 76071 and 78137, respectively. The hardness was measured at regular 50 µm intervals from the edge of the spring section toward the core (to approximately 1/4 the diameter of the spring from its OD). The hardnesses of the core regions were determined by taking mean hardness values from four points in the center.

The mean hardness both at the edge and in the core for both samples were very similar. No significant variation in hardness was found at the edge of either sample. Sample 76071 had a mean hardness of 577 HV (Vickers hardness) at the edge, and 571 HV at the core. Sample 78137 had a mean hardness of 582 HV at the edge, and 552 HV at the core. These

hardnesses are equivalent to ~54 HRC (Rockwell C scale). These hardnesses are consistent with the results found in the Haldex springs.

No evidence of local surface hardening was found. It is apparent that shot peening has not been performed, or that the material has been subsequently altered to remove the peened layer. The lack of this compressive stress surface layer means that the spring would have a lower resistance to fatigue crack initiation compared to a shot peened surface.

MATERIALS CHEMISTRY

Table 2 shows the results of optical emission spectroscopy examination for each of the spring samples sent.

Silicon (Si) and chromium (Cr) additions in springs are used for anti-relaxation. The presence of chromium increases corrosion resistance, but not significantly at this low level.

The composition of both samples is consistent with that of the Haldex springs, with the exception of the presence of aluminum (Al) in these samples, and additional copper (Cu).

ELECTRON MICROSCOPY/ENERGY DISPERSIVE SPECTROCOPY

The black deposits found on the fracture surface of Sample 76071 D were analyzed using the scanning electron microscope (SEM) and x-ray energy dispersive spectroscopy (X-EDS) to determine the elemental composition of the deposit. A SEM image map of the locations of compositional analysis of the black deposit on Sample 76071 D is given in Figure 25 (A).

The results of the analysis from a region along the lower lip of the fracture surface are shown in the X-EDS spectra in Figure 25 (B). The deposit mostly consists of aluminum, oxygen, and silicon, with isolated regions also high in carbon (C). The source of the aluminum and oxygen is likely the oxidized interior surface of the chamber upon which the sharp spring edge likely rubbed post fracture. The source of the silicon and carbon is not clear, but could conceivably be debris from the environment that entered the unsealed chamber in service or during laboratory testing. The deposit is on the fracture surface of the spring steel. No corrosion of the steel was

observed local to the black deposit. This supports the theory that the material was deposited post-fracture of the spring and did not contribute to this failure.

CONCLUSIONS

- The primary failure mode of both samples supplied was torsional fatigue initiated at a corrosion pit on the spring OD, caused by corrosion of the exposed steel in the environment in regions where the paint had de-bonded from the spring surface.

- The polymer coating is only present in patches on the surface of the segments provided. The metal exposed where the paint is not present appears to be oxidized and pitted. The likely cause of the corrosion was interaction with the potentially wet and corrosive (e.g., road salt) environment that the vehicle was subjected to in service. In general, the state of the coated surface appeared similar to that on the Haldex springs. Large areas of coating were missing, and the majority of these areas showed corrosion of the underlying spring steel.

- Several of the fracture surfaces had evidence of mechanical wear, likely a result of the two adjacent fracture surfaces rubbing together while held loosely in place post-spring fracture and pre-diaphragm rupture. It is also possible that the broken spring sections could have made contact with the interior parts of the brake chamber. The remainder of the chamber was not supplied to Intertek AIM for evaluation, so this cannot be confirmed.

- A black deposit was observed on the fracture surface of several of the spring segments supplied for Sample 76071 in regions where the spring was at its widest (“beehive” shape). X-EDS revealed that the deposit mostly consisted of aluminum, oxygen, and silicon, with isolated regions also high in carbon. The brake chamber was made of aluminum, and was oxidized according to VRTC observations. The source of the aluminum and oxygen is likely the oxidized interior surface of the chamber upon which the sharp spring edge probably rubbed post fracture. The source of the silicon and carbon is not clear, but could conceivably be debris from the environment that entered the unsealed chamber in service or during laboratory testing. The deposit is on the fracture surface of the spring steel. No corrosion of the steel was observed local to the

black deposit. This supports the theory that the material was deposited post-fracture of the spring, and did not contribute to its failure.

- The microstructure of the spring steel is consistent with that of lightly tempered martensite. This is also consistent with that of the Haldex springs and their manufacturing specification.

- The compositions of the spring samples are consistent with one another and appear to be very similar to those of the Haldex springs.

- No evidence of case hardening or shot peening was found in either of the spring samples supplied. The hardness of the samples appears very consistent from the core to the edge of the sample. Hardnesses were consistent with those found in the Haldex springs.

Table 1

EXAMINATION DETAILS – CHAMBERS 76071 AND 78137

	Carrier Info		Initial Inspection				Cycle Test		Comments
	Unit No.	VIN	Type	Drop Test Sound	Exterior Inspection Comments	Actuator Pushrod Position	Cycles to Failure	Cycles with Broken Spring	
In-service Peer Chambers	76071	Peer MGM #1	30LP3	spring vibration	used	straight	66,829 cycles power spring fractured, 68,444 cycles spring break #2, 85,155 air leak at diaphragm	18,326	cycle test #15
	78137	Peer MGM #2	30LP3	spring vibration	used	straight	61,065 cycles power spring fractured, 62,480 cycles air leak at diaphragm	1,415	cycle test #14

Table 2

CHEMICAL COMPOSITIONAL ANALYSIS BY OPTICAL EMISSION SPECTROSCOPY (* By LECO Combustion)

Element	Composition 76071 (wt. %)	Composition 78137 (wt. %)
Aluminum (Al)	0.02	0.02
Carbon* (C)	0.56	0.56
Chromium (Cr)	0.70	0.69
Copper (Cu)	0.70	0.69
Manganese (Mn)	0.70	0.69
Molybdenum (Mo)	0.01	0.01
Nickel (Ni)	0.02	0.02
Phosphorus (P)	0.011	0.009
Silicon (Si)	1.44	1.43
Sulfur* (S)	<0.005	<0.005
Vanadium (V)	<0.005	<0.005
Iron (Fe)	Balance	Balance



Figure 1 — As-received – General.



Figure 2 — As-received – General – 76071.

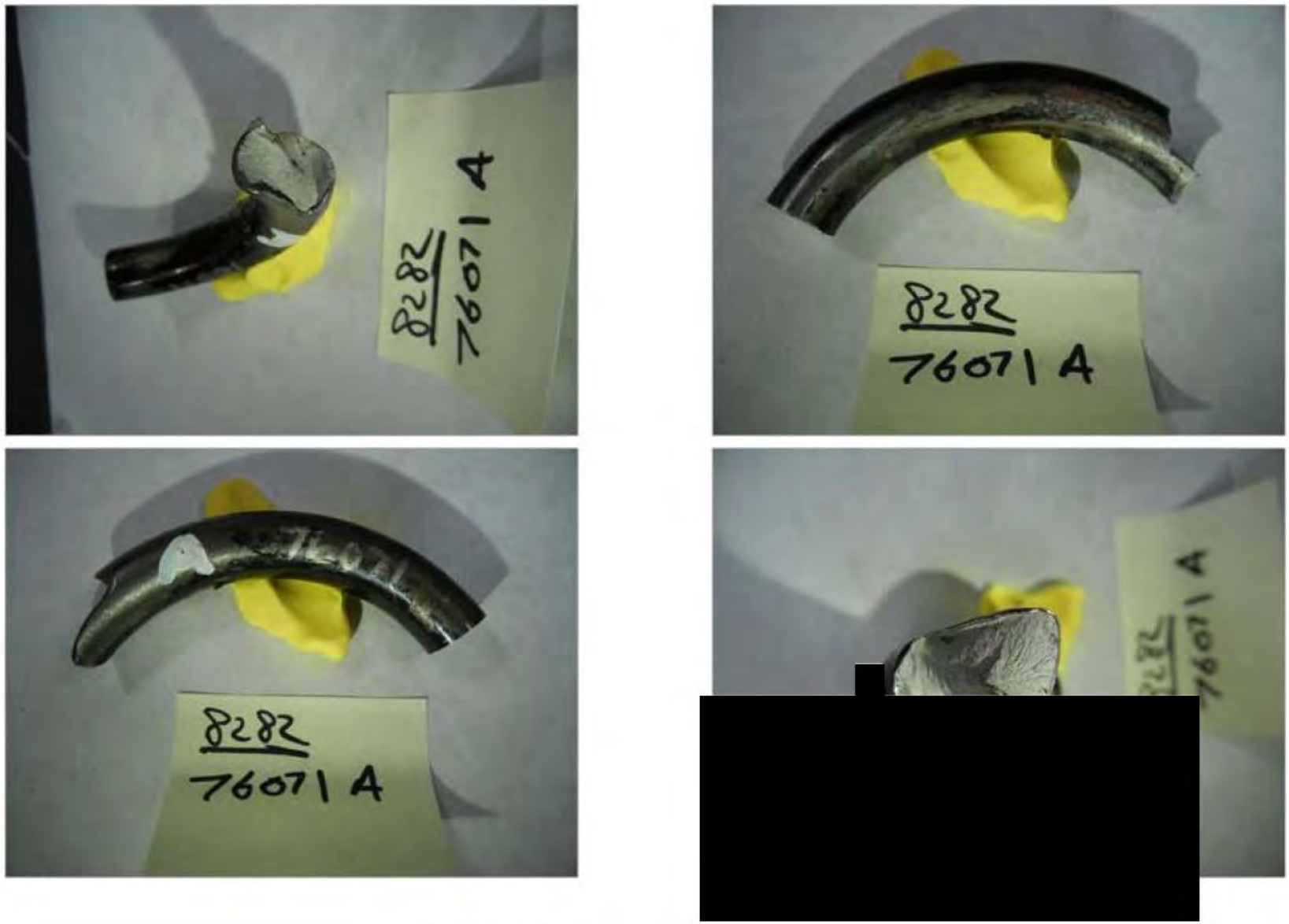


Figure 3 — As-received – Individual: 76071 A.

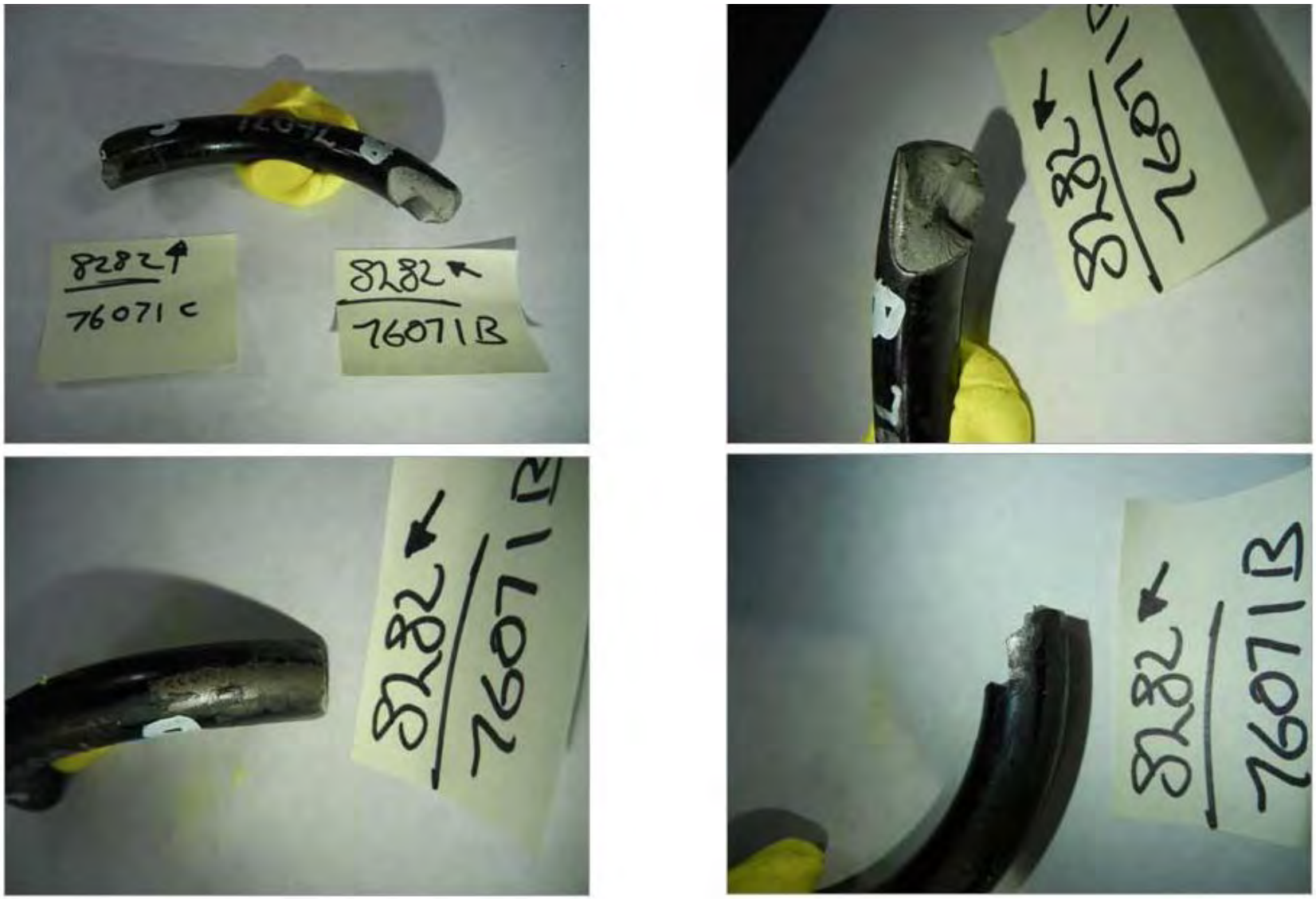


Figure 4 — As-received – Individual: 76071 B.



Figure 5 — As-received – Individual: 76071 C.



Figure 6 — As-received – Individual: 76071 D.



Figure 7 — As-received – Individual: 76071 E.

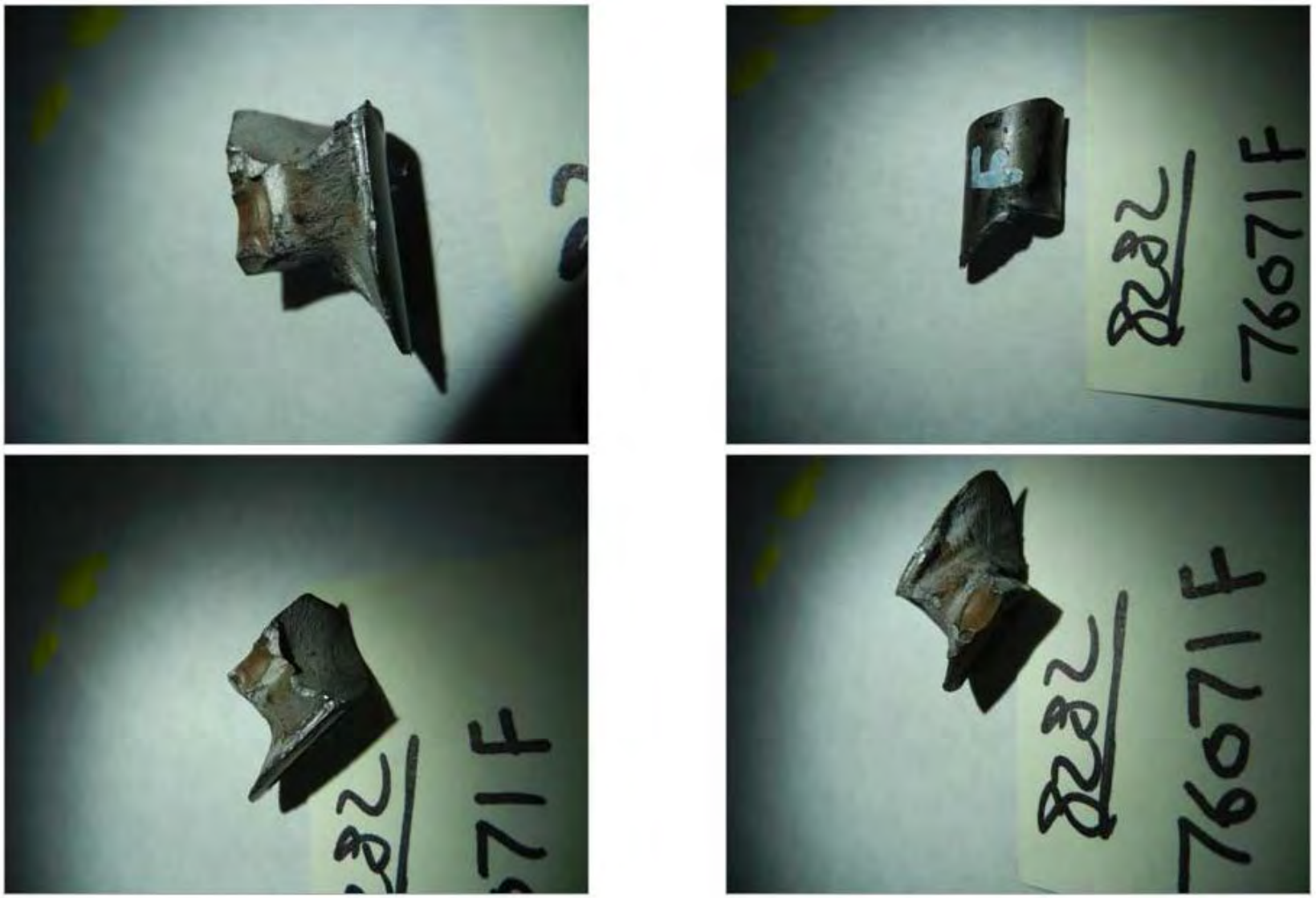


Figure 8 — As-received – Individual: 76071 F.



Figure 9 — As-received – Individual: 76071 G.



Figure 10 — As-received – Individual: 78137 A.



Figure 11 — As-received – Individual: 78137 B.

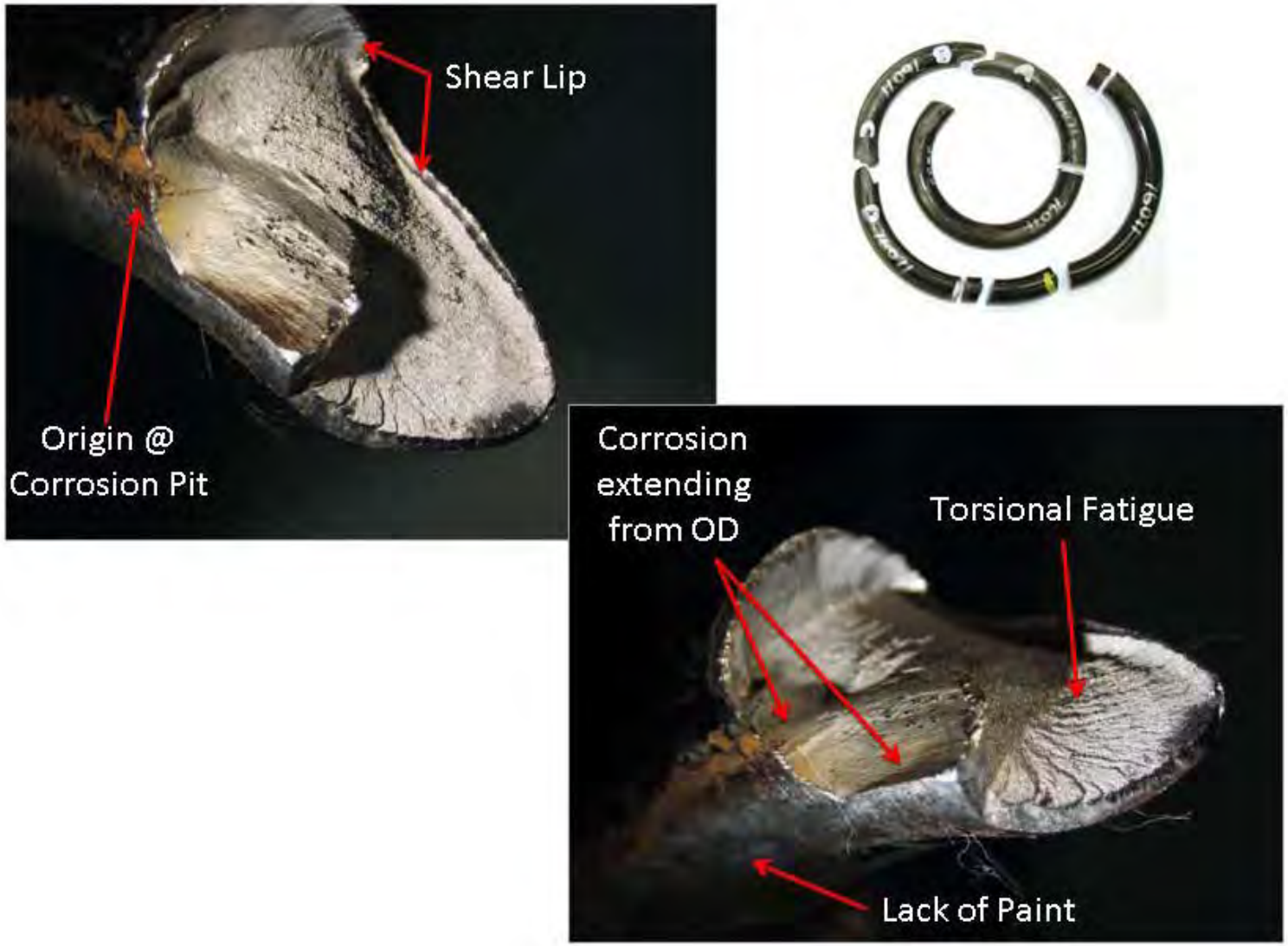


Figure 12 — Fracture Surface – 76071 A.

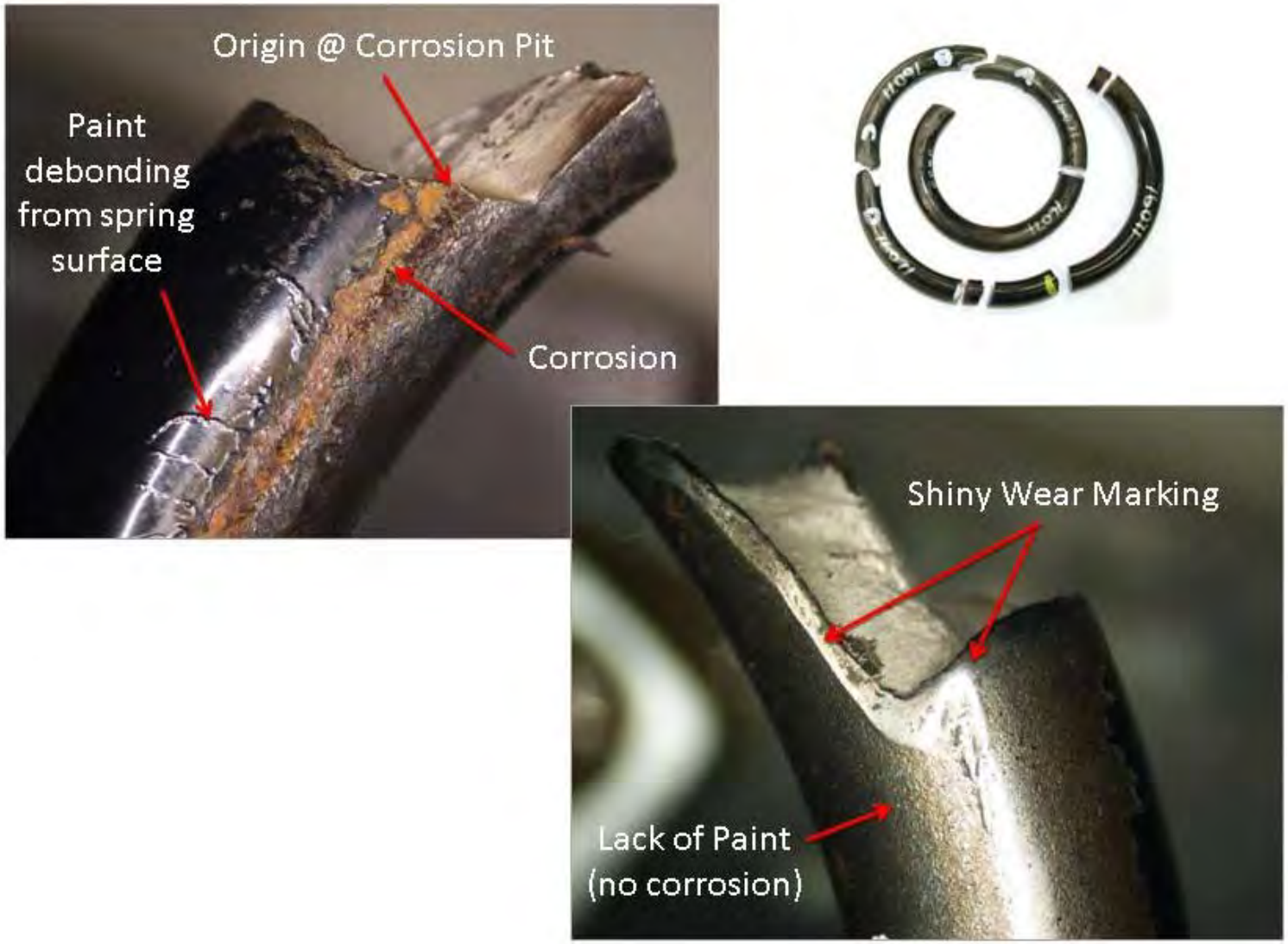


Figure 13 — Fracture Surface – 76071 A.

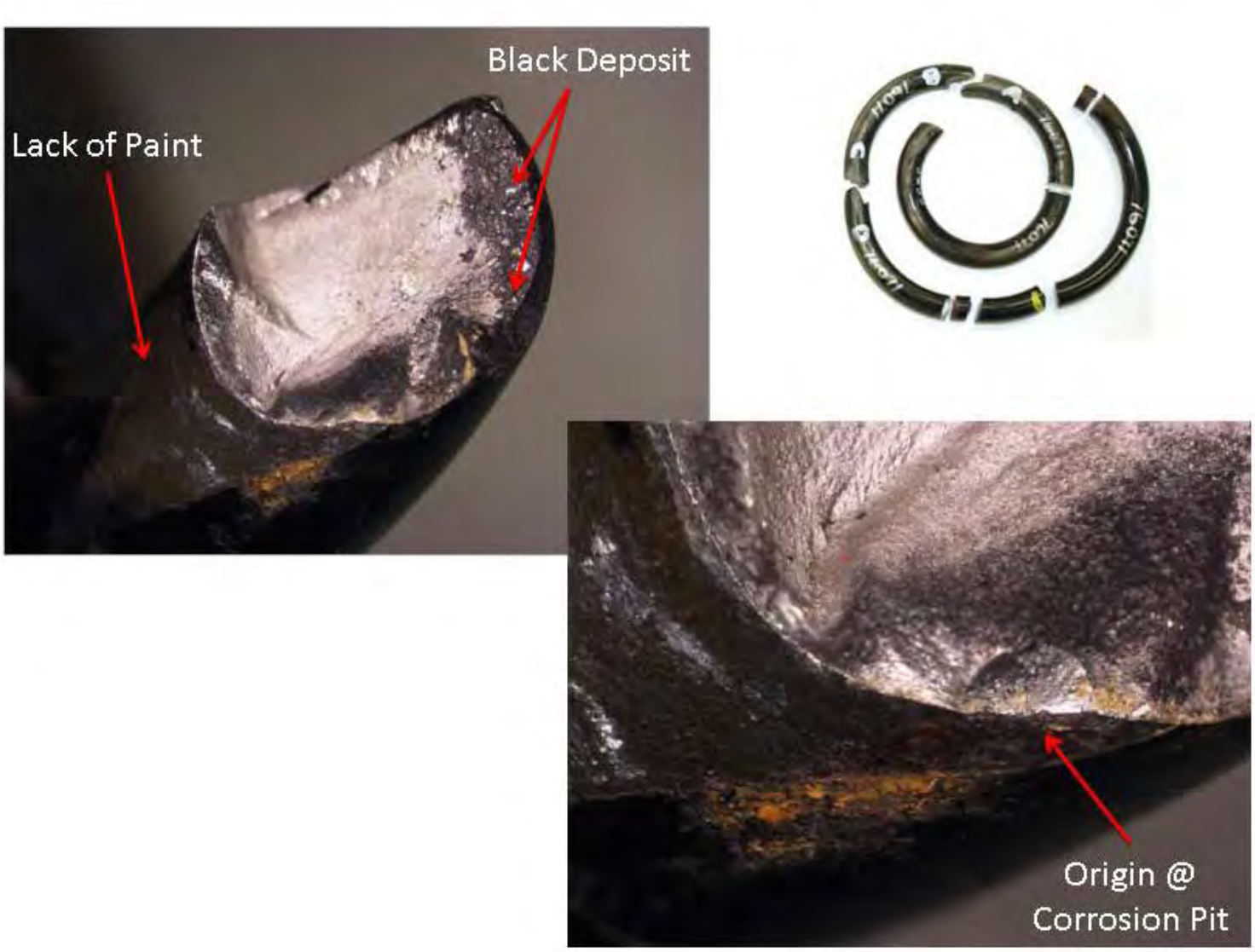


Figure 14 — Fracture Surface – 76071 D.

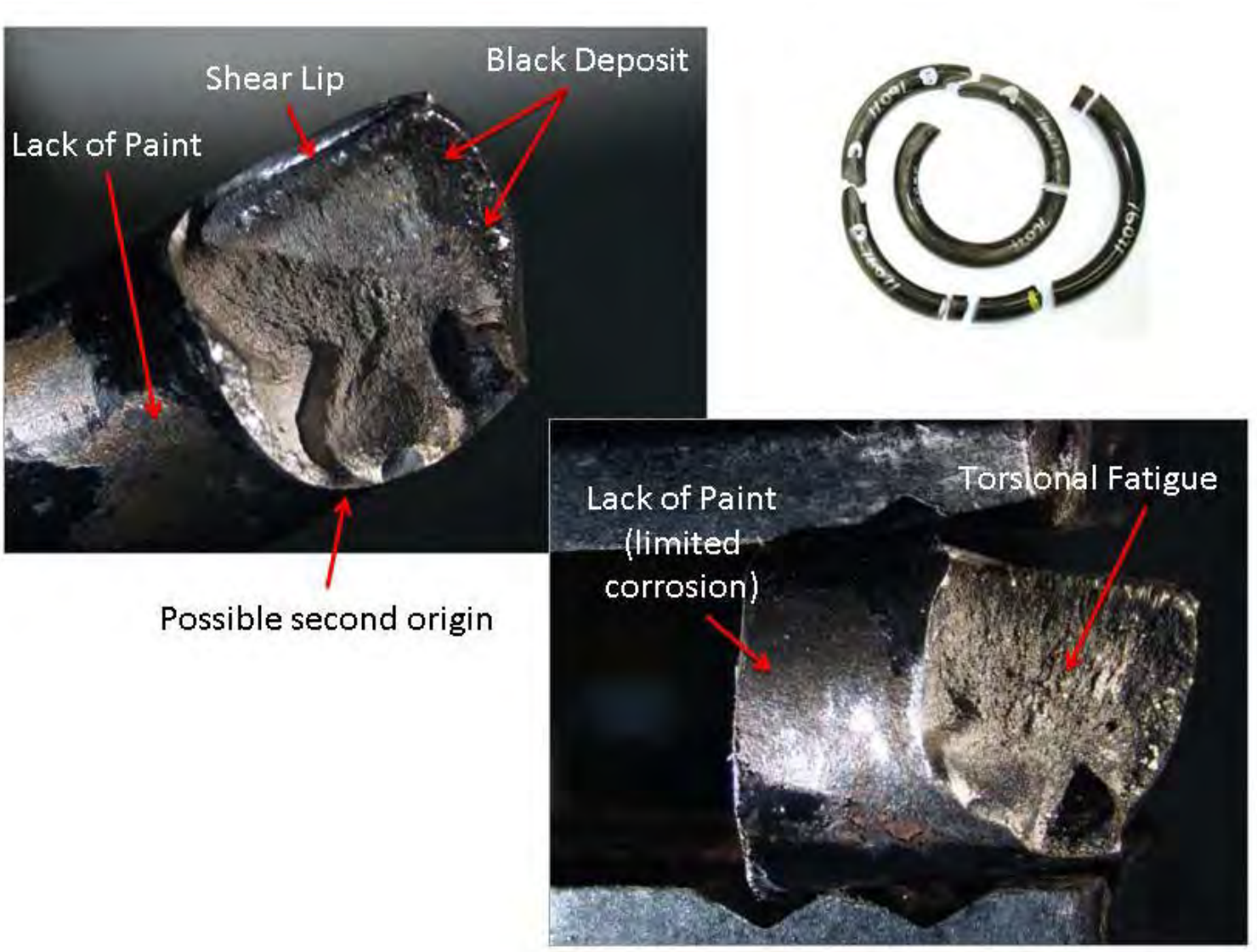


Figure 15 — Fracture Surface – 76071 D.

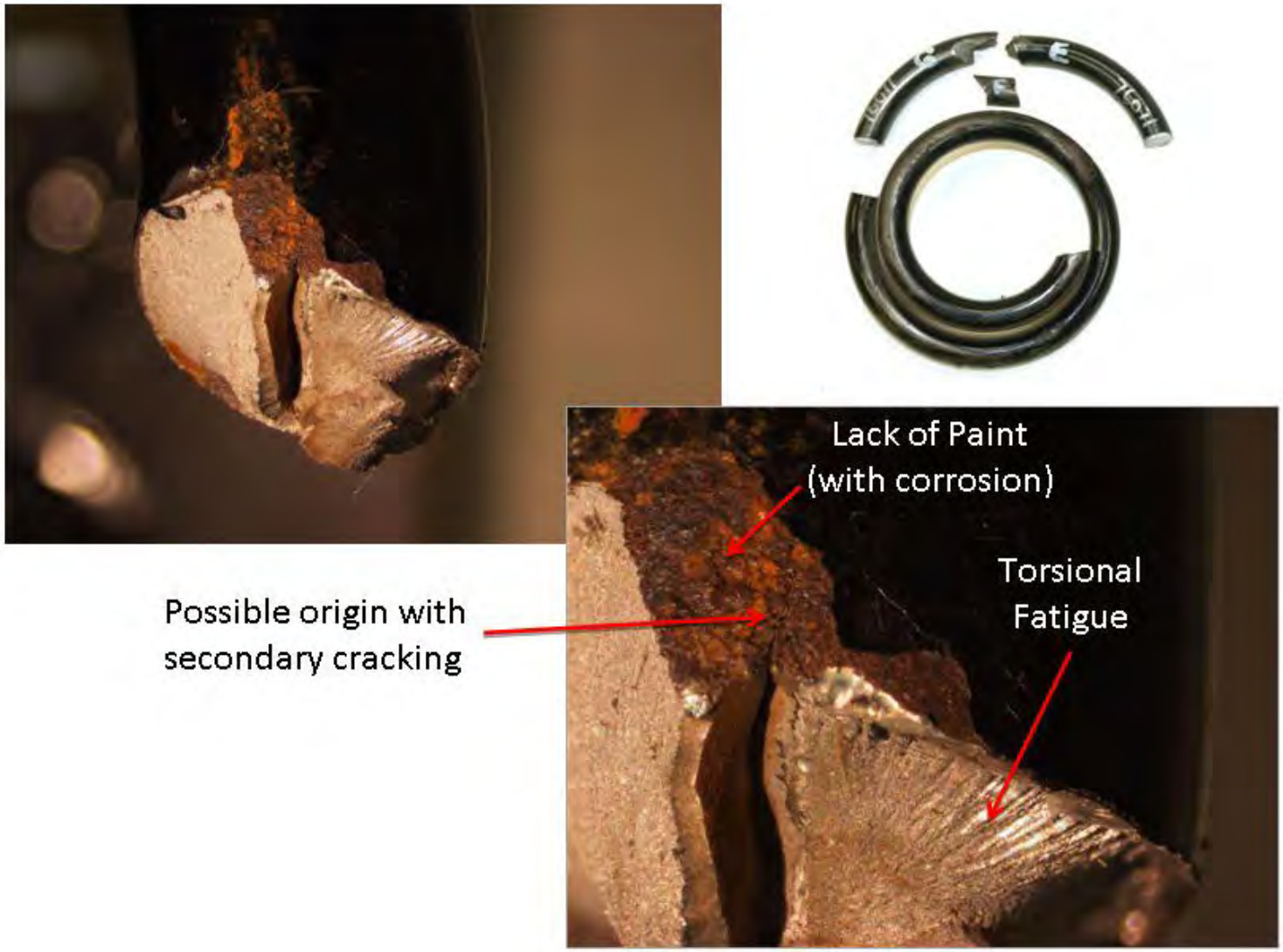


Figure 16 — Fracture Surface – 76071 E.

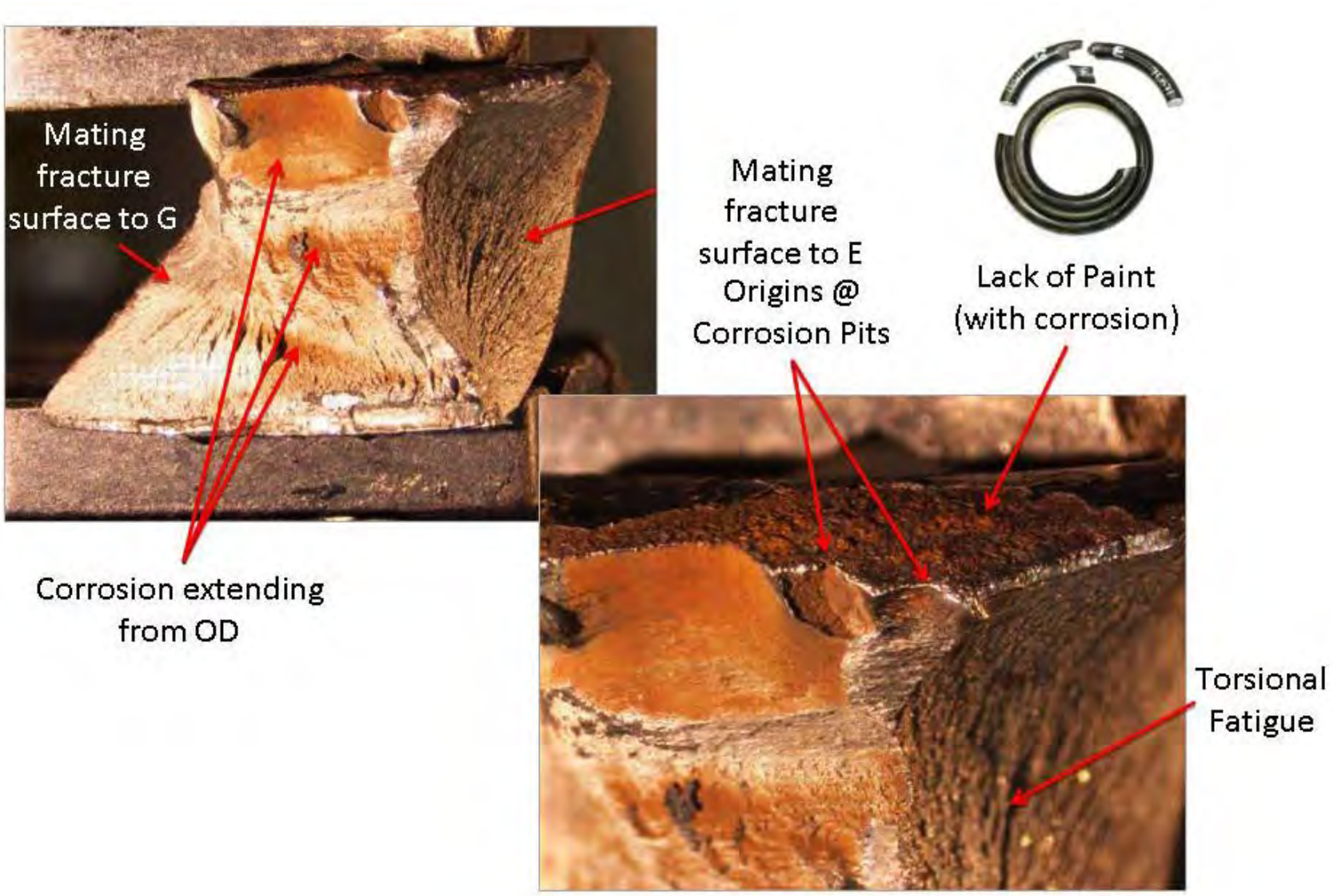


Figure 17 — Fracture Surface – 76071 F.

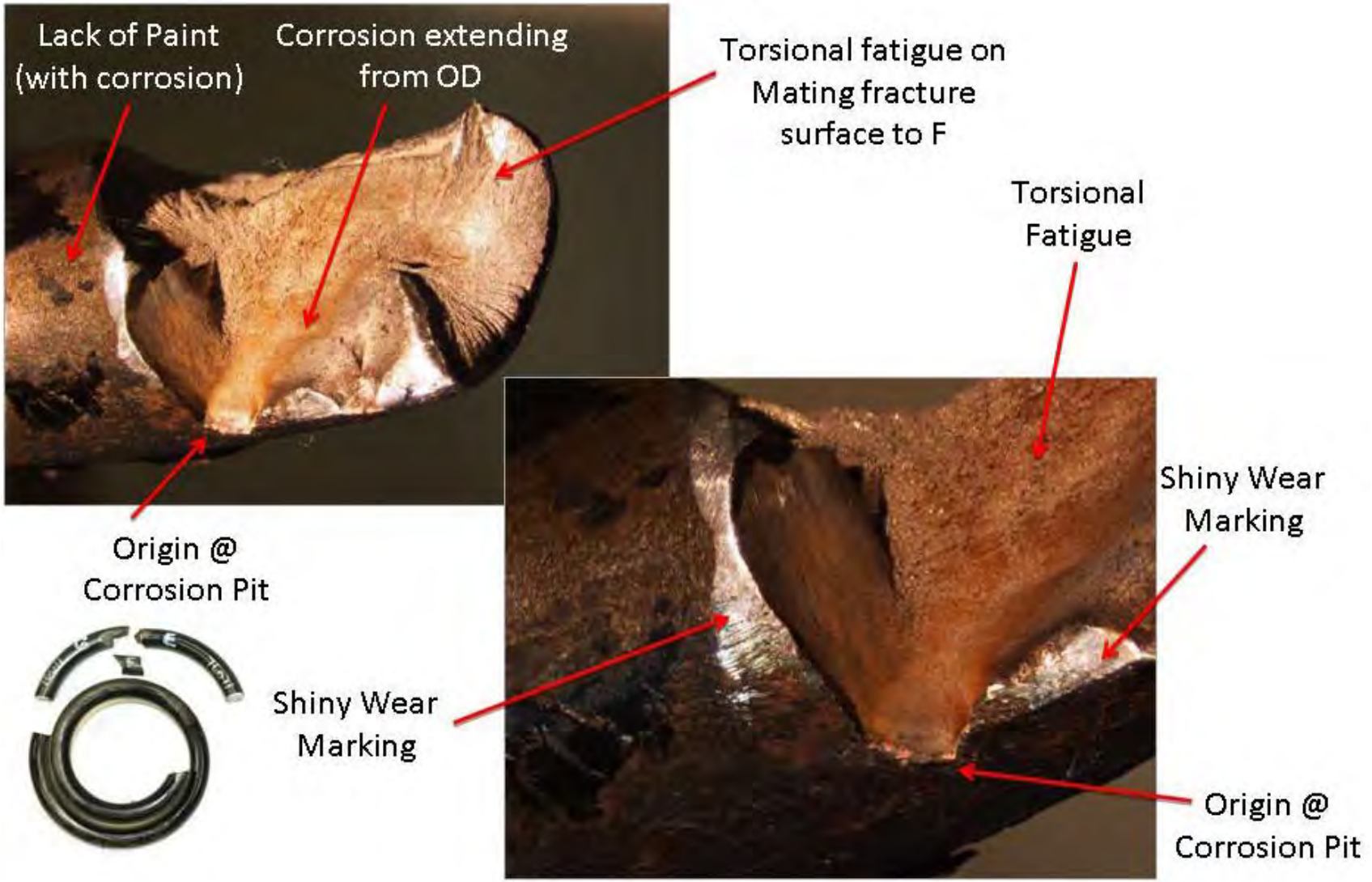


Figure 18 — Fracture Surface – 76071 G.

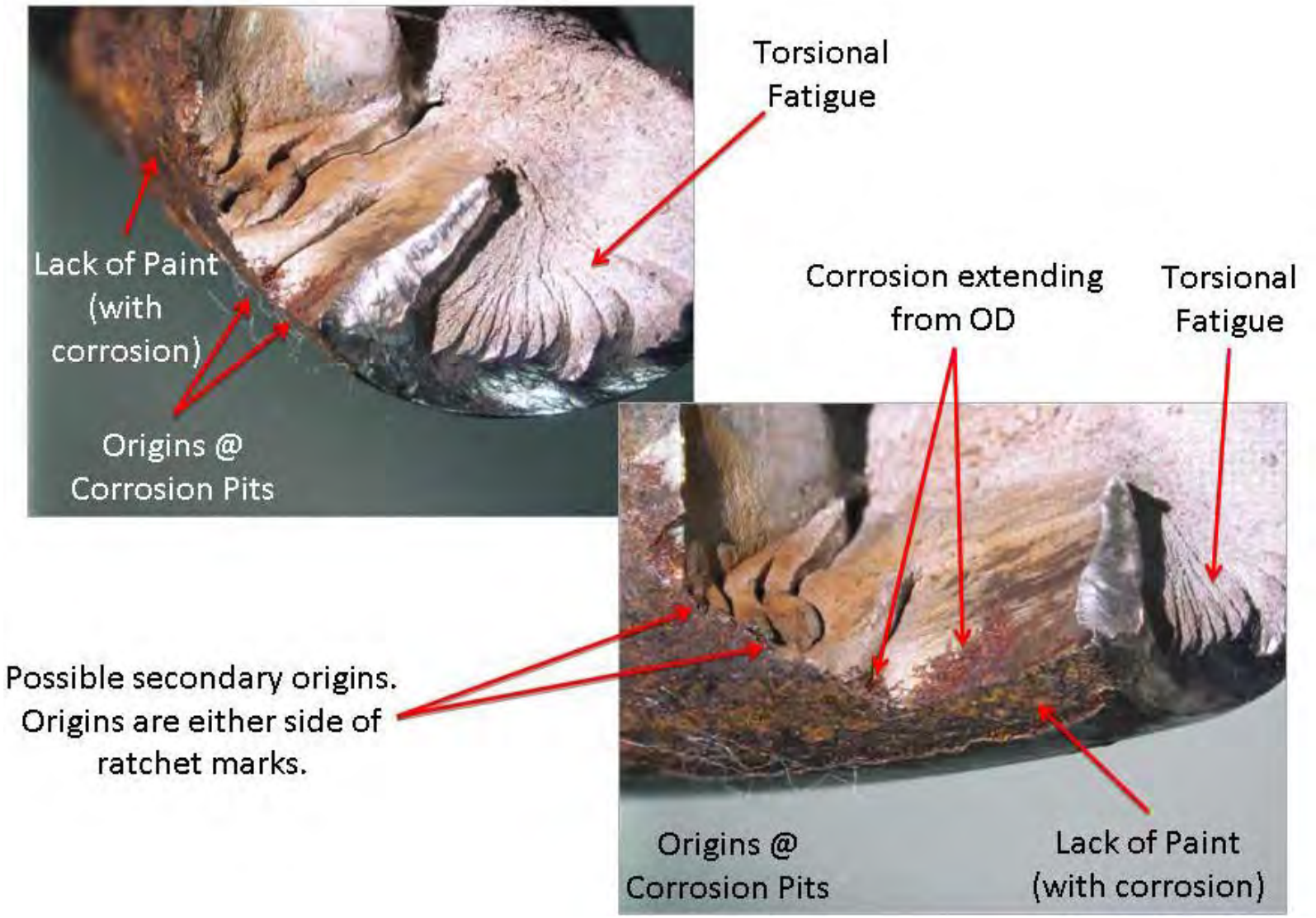


Figure 19 — Fracture Surface – 78137 A.

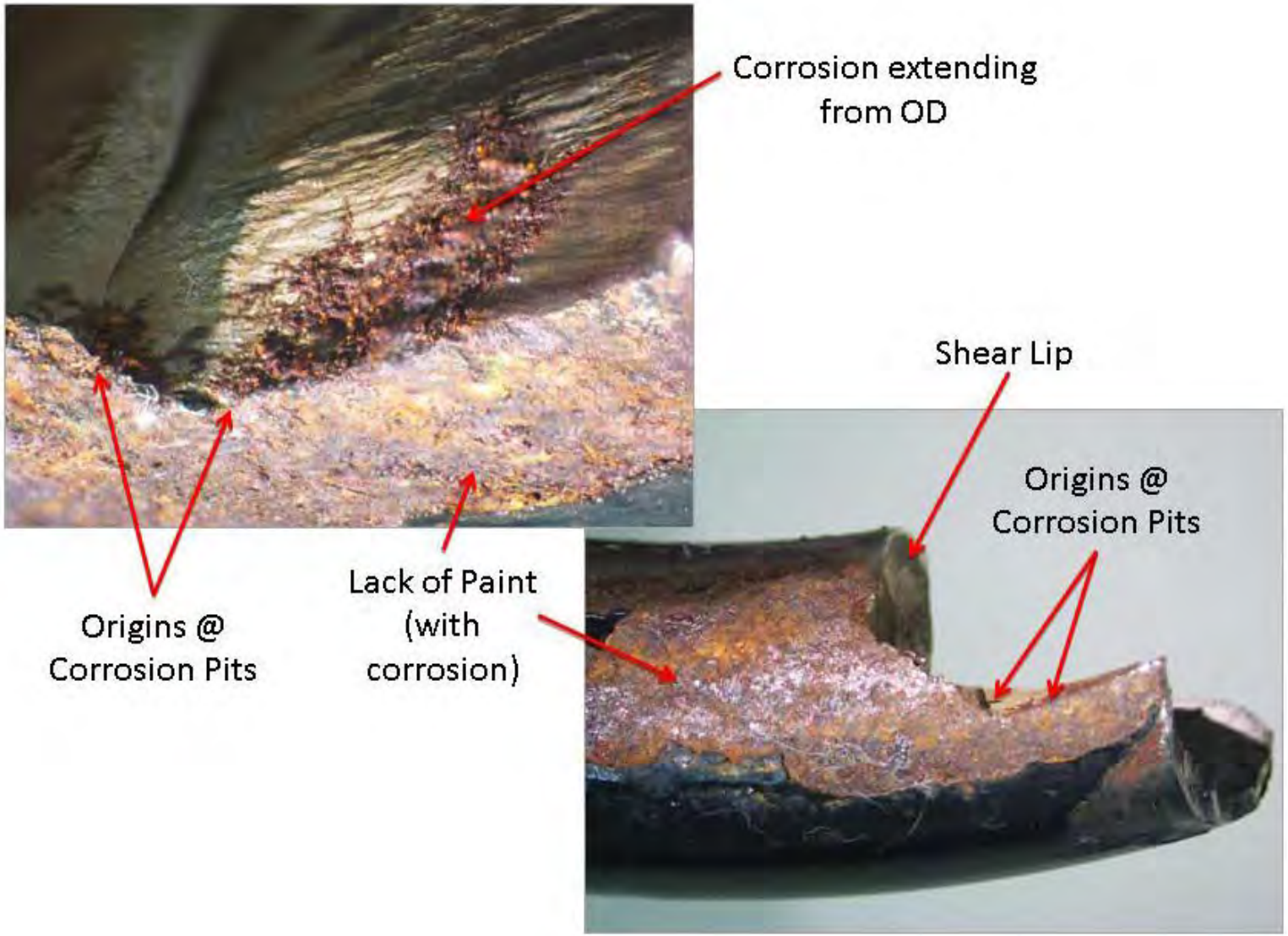


Figure 20 — Fracture Surface – 78137 A.

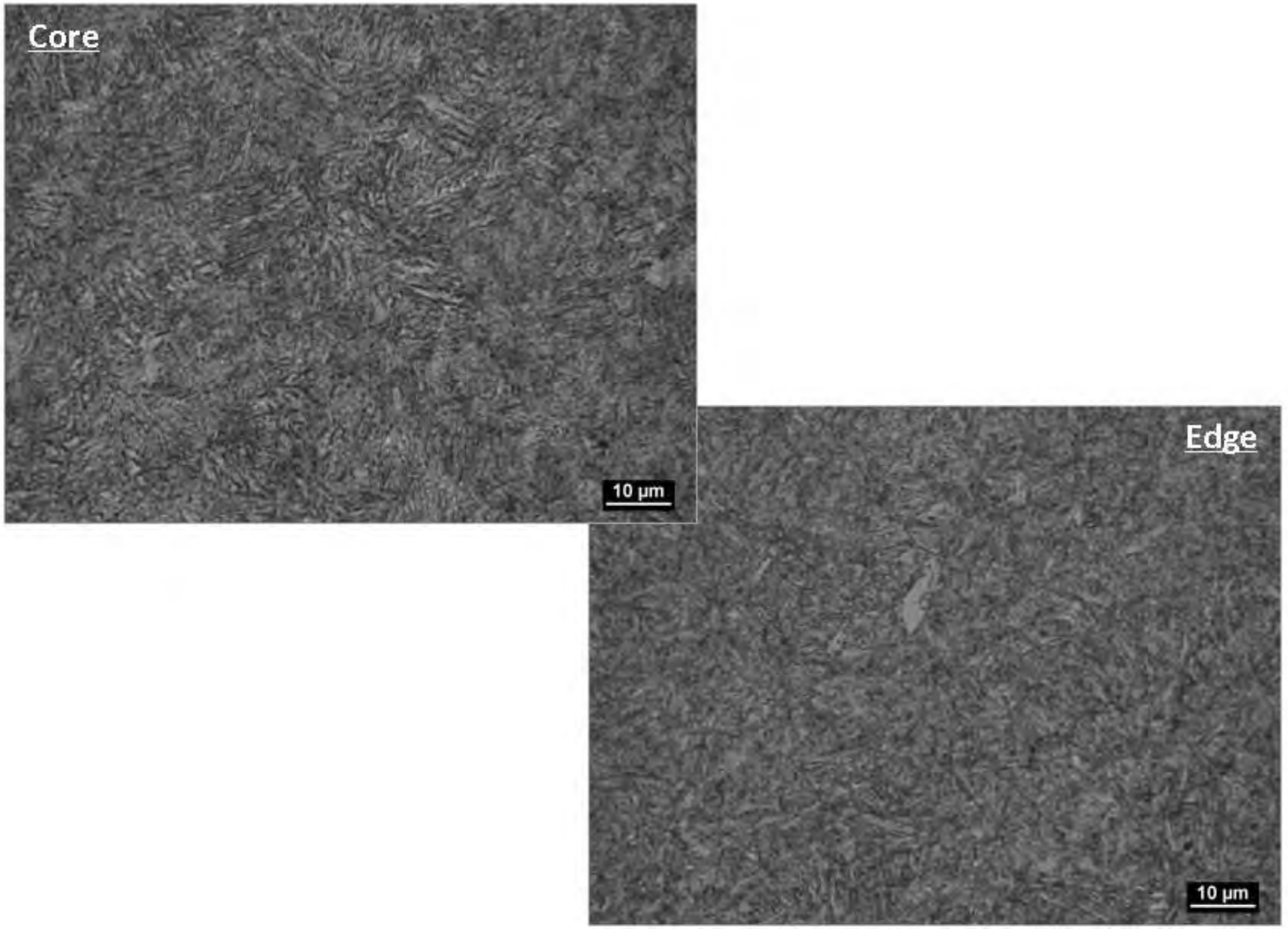


Figure 21 — Microstructure (4% Nital Etch) – MAG: 1,000X – 76071.

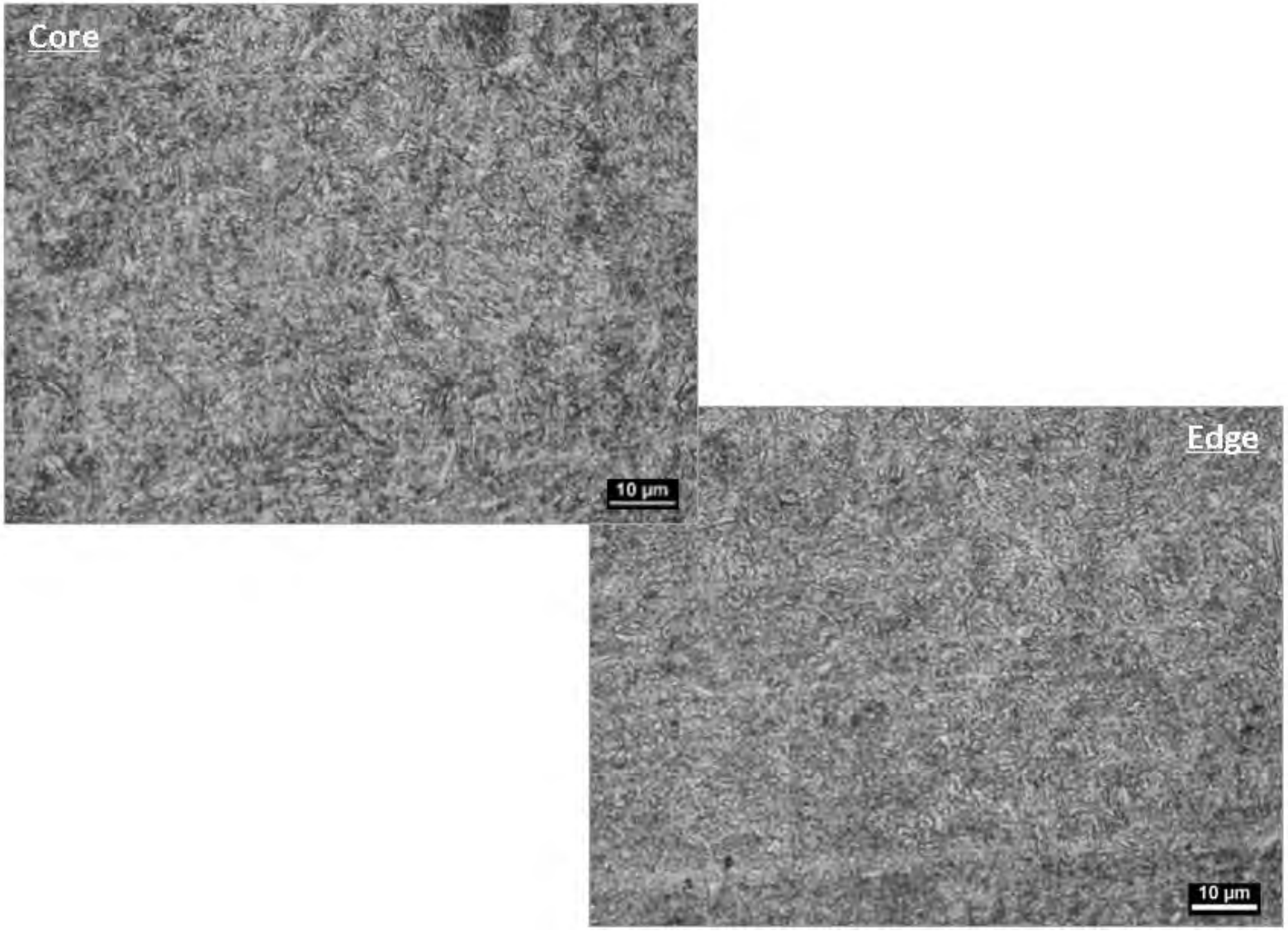


Figure 22 — Microstructure (4% Nital Etch) – MAG: 1,000X – 78137.

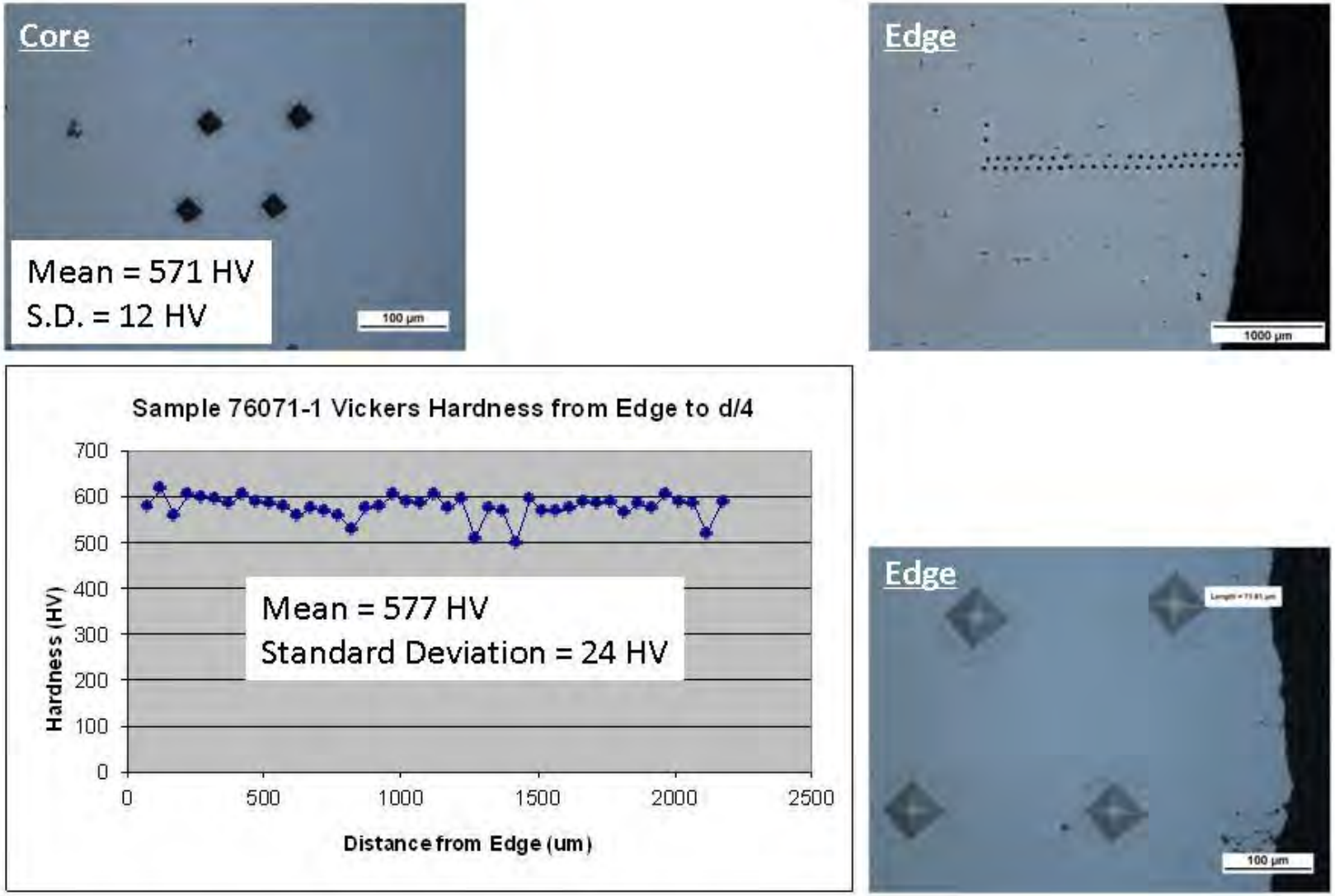


Figure 23 — Microhardness Traverse – 76071 (Taken from the Edge Toward the Core to ~1/4 of the Diameter of the Spring Section).

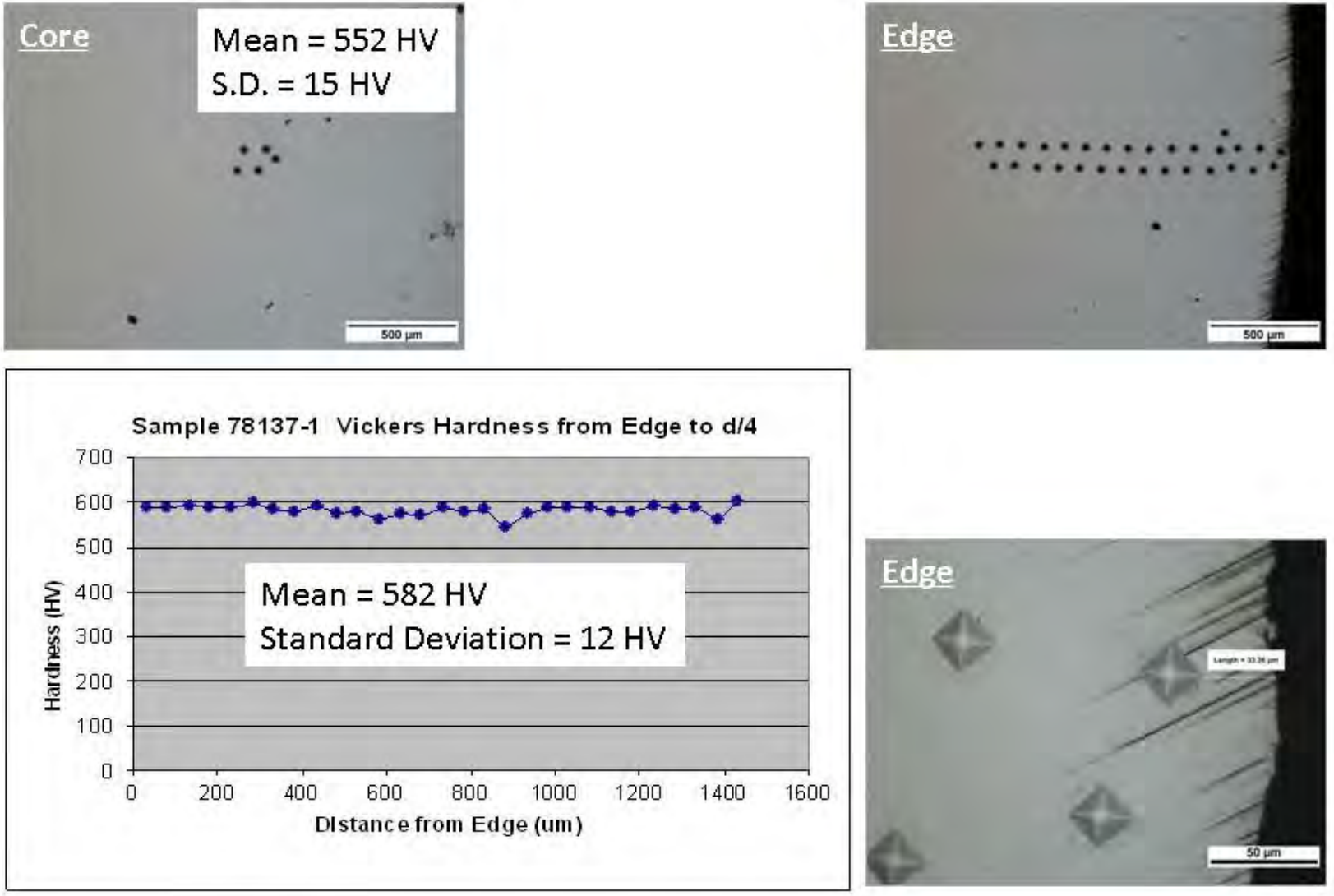


Figure 24 — Microhardness Traverse – 78137 (Taken from the Edge Toward the Core to ~1/4 of the Diameter of the Spring Section).

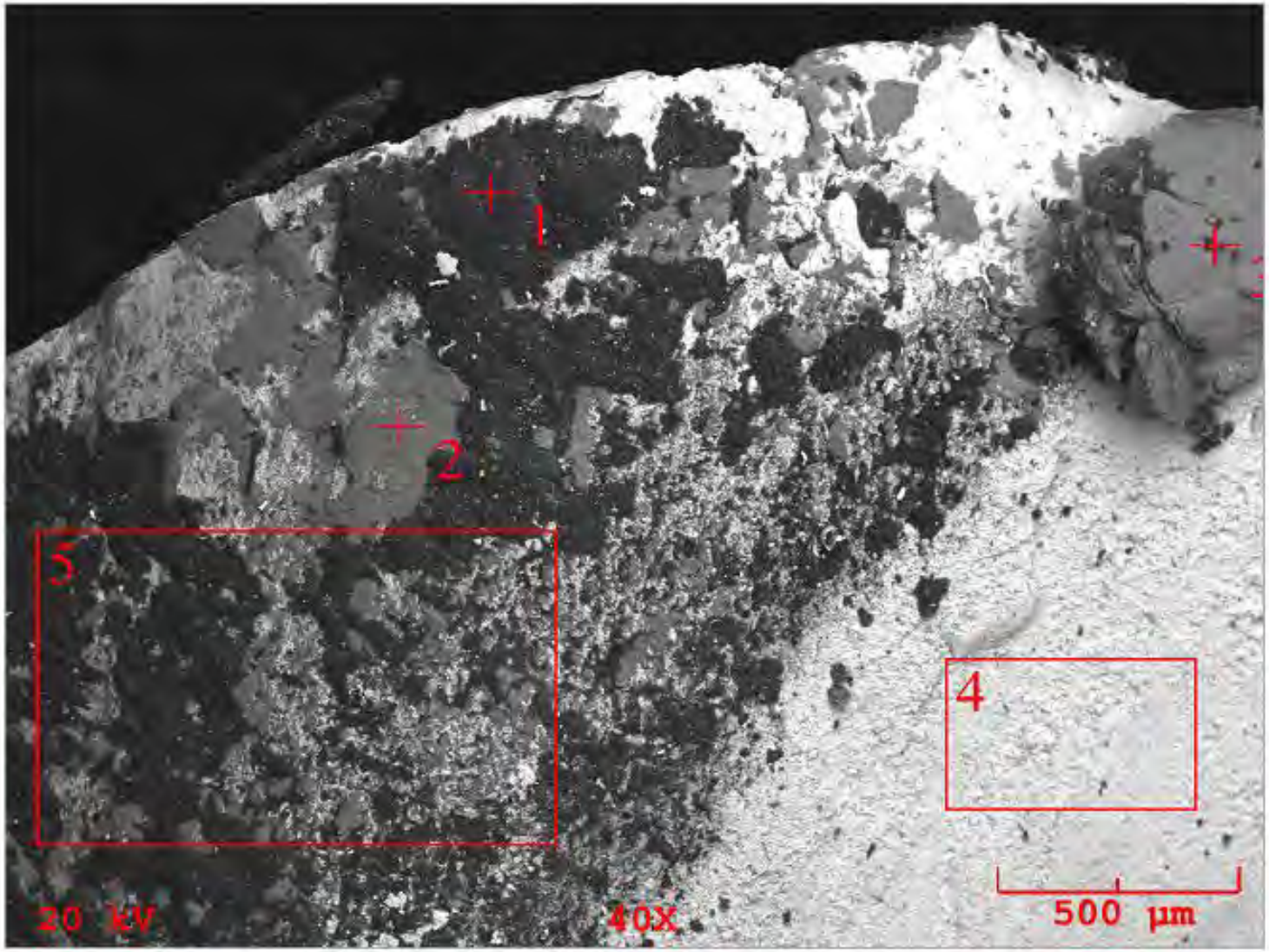


Figure 25 (A) — Map of Locations of Compositional Analysis of Black Deposit on 76071 D on the Lower Lip of the Fracture Surface.

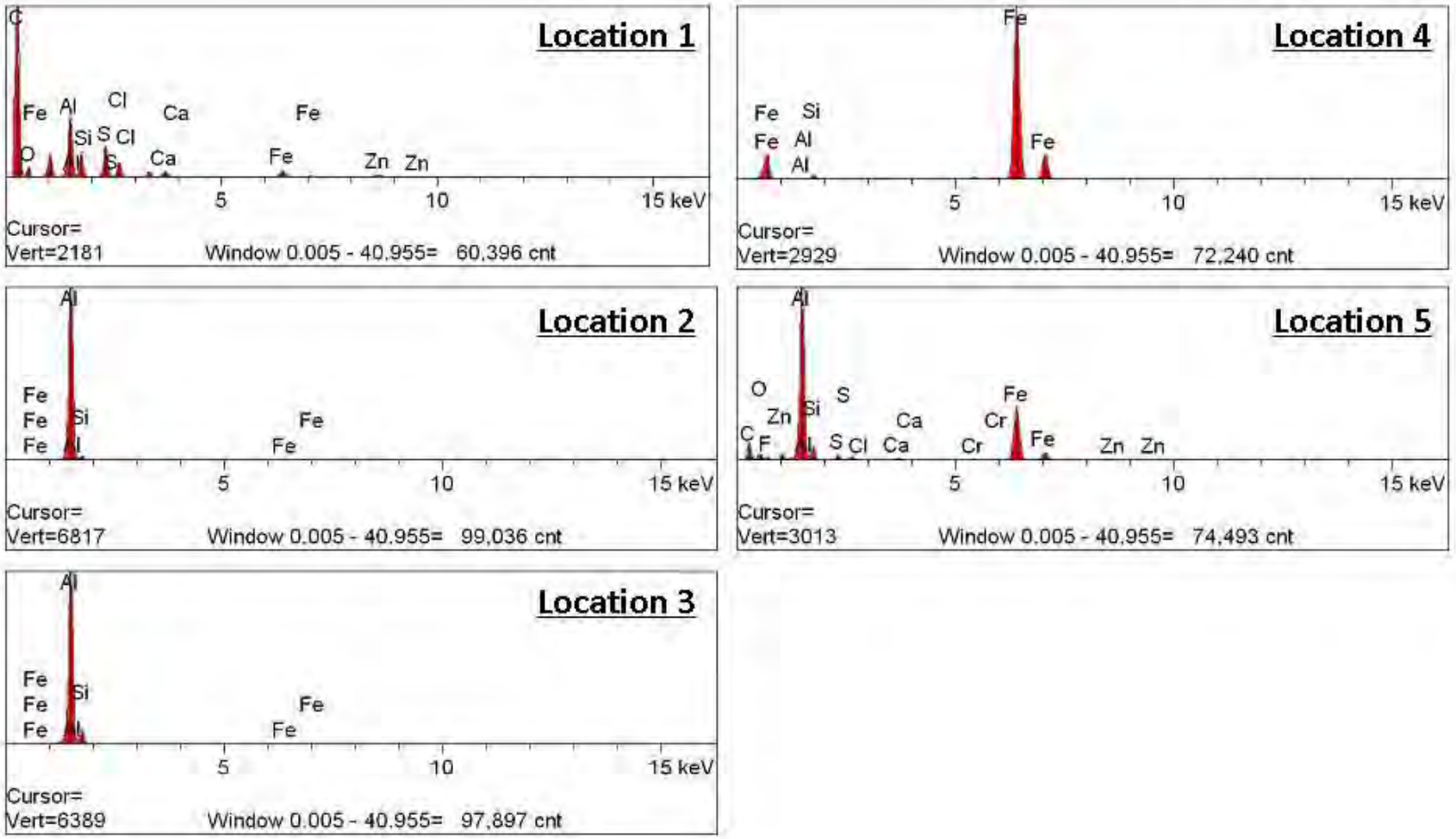


Figure 25 (B) — Compositional Analysis of Black Deposit on 76071 D on the Lower Lip of the Fracture Surface.

Offices

16100 Cairnway Drive, Suite 310
Houston, TX 77084
Phone: 832.593.0550
Fax: 832.593.0551
Toll Free: 800.568.3201

601 West California Avenue
Sunnyvale, CA 94086
Phone: 408.745.7000
Fax 408.734.0445

139, 11215 Jasper Avenue
Edmonton, AB T5K 0L5
Canada
Phone: 780.669.2869
Fax: 780.669.2509

www.intertek.com/aim